

Direct Coulomb explosion of N_2O^{2+} induced by monochromatic extreme ultraviolet photons at 38.5 eV

Min Zhang(张敏), B Najjari, Bang Hai(海帮), Dong-Mei Zhao(赵冬梅), Jian-Ting Lei(雷建廷), Da-Pu Dong(董达谱), Shao-Feng Zhang(张少锋), Xin-Wen Ma(马新文)

Citation: Chin. Phys. B . 2020, 29(6): 063302 . **doi:** 10.1088/1674-1056/ab8629
Journal homepage: http://cpb.iphy.ac.cn; http://iopscience.iop.org/cpb

What follows is a list of articles you may be interested in

Field-free molecular orientation steered by combination of super-Gaussian and THz half-cycle laser pulses

Qi-Yuan Cheng(程起元), Yu-Zhi Song(宋玉志), Qing-Tian Meng(孟庆田)

Chin. Phys. B . 2019, 28(11): 113301 . **doi:** 10.1088/1674-1056/ab4cdf

Influence factor analysis of field-free molecular orientation

Jing-Song Liu(刘劲松), Qi-Yuan Cheng(程起元), Da-Guang Yue(岳大光), Xu-Cong Zhou(周旭聪), Qing-Tian Meng(孟庆田)

Chin. Phys. B . 2018, 27(3): 033301 . **doi:** 10.1088/1674-1056/27/3/033301

Numerical analyses on optical limiting performances of chloroindium phthalocyanines with different substituent positions

Yu-Jin Zhang(张玉瑾), Xing-Zhe Li(李兴哲), Ji-Cai Liu(刘纪彩), Chuan-Kui Wang(王传奎)

Chin. Phys. B . 2016, 25(1): 013302 . **doi:** 10.1088/1674-1056/25/1/013302

Interferences in photo-detached electron spectra froma non-collinear tri-atomic anion

A. Afaq, K. Farooq, M. A. Khan, Yi Xue-Xi

Chin. Phys. B . 2014, 23(10): 103304 . **doi:** 10.1088/1674-1056/23/10/103304

Field-free molecular orientation induced by combined femtosecond single- and dual-color laser pulses：The role of delay time and quantum interference

Qin Chao-Chao, Jia Guang-Rui, Zhang Xian-Zhou, Liu Yu-Fang, Long Jin-You, Zhang Bing

Chin. Phys. B . 2014, 23(1): 013302 . **doi:** 10.1088/1674-1056/23/1/013302

Direct Coulomb explosion of N_2O^{2+} induced by monochromatic extreme ultraviolet photons at 38.5 eV*

Min Zhang(张敏)[1,2], B Najjari[1], Bang Hai(海帮)[1,2], Dong-Mei Zhao(赵冬梅)[1,2], Jian-Ting Lei(雷建廷)[3], Da-Pu Dong(董达谱)[1,2], Shao-Feng Zhang(张少锋)[1,2,†], and Xin-Wen Ma(马新文)[1,2,‡]

[1] *Institute of Modern Physics, Chinese Academy of Sciences, Lanzhou* 730000, *China*
[2] *University of Chinese Academy of Sciences, Beijing* 100049, *China*
[3] *School of Nuclear Science and Technology, Lanzhou University, Lanzhou* 730000, *China*

(Received 27 February 2020; revised manuscript received 31 March 2020; accepted manuscript online 3 April 2020)

The direct Coulomb explosion of N_2O^{2+} has been investigated experimentally after double-ionization by a single extreme ultraviolet (EUV) photon with an energy of ~ 38.5 eV. From the ion–ion time-of-flight coincidence spectrum, the de-nitrogenation ($N_2O^{2+} \rightarrow N^+ + NO^+$) and de-oxygenation ($N_2O^{2+} \rightarrow O^+ + N_2^+$) photodissociation channels of N_2O^{2+} are unequivocally identified. The measured kinetic energy release (KER) distribution of the de-nitrogenation channel presents a major peak accompanied by a shoulder structure. We find that the major peak can be attributed to the direct photodissociation of the $1^1\Delta$ and $1^1\Sigma^+$ states, while the shoulder structure should be ascribed to the predissociation of the $1^1\Delta$ and $1^1\Sigma^+$ states via $1^3\Pi$ state.

Keywords: extreme ultraviolet photon, kinetic energy release, photodissociation pathway

PACS: 33.80.–b **DOI:** 10.1088/1674-1056/ab8629

1. Introduction

N_2O is very stable in the troposphere and its global warming potential is about 300 times higher than that of CO_2.[1] Even worse, after transported to the stratosphere, N_2O can release active nitrogen oxides (NO) via the de-nitrogenation process induced by the solar radiation or charged particles from the space.[2] There, NO catalytically destroys the ozone layer. In fact, it is found that the agricultural practices and the use of N-fertilizers have already greatly enhanced emissions of N_2O for the last two decades[3] which is becoming the largest ozone-depleting emission in the 21st century.[2] Studies on the de-nitrogenation processes of N_2O in presence of external fields are thus of significance in the air pollution control and attract more and more attentions.[4,5]

A non-negligible de-nitrogenation channel originating from the Coulomb explosions of N_2O^{2+} has been reported recently.[5,6] After removal of two electrons from N_2O induced by the solar radiation or charged particles from the space, the molecular dication N_2O^{2+} subsequently dissociates through four different fragmentation channels as follows:[6–9]

$$N_2O^{2+} \rightarrow N^+ + NO^+ \quad (E_L = 28.8\ \text{eV}), \tag{1}$$

$$N_2O^{2+} \rightarrow O^+ + N_2^+ \quad (E_L = 30.9\ \text{eV}), \tag{2}$$

$$N_2O^{2+} \rightarrow N^+ + O^+ + N \quad (E_L = 39.6\ \text{eV}), \tag{3}$$

$$N_2O^{2+} \rightarrow N^+ + N^+ + O \quad (E_L = 40.6\ \text{eV}), \tag{4}$$

where E_L is the corresponding lowest adiabatic threshold energy. NO^+ produced in channel (1) and those induced by channels (2)–(4) can be neutralized subsequently by the surrounding atmosphere molecules and enter into the ozone depleting processes. Hence, detailed information on its ionization or dissociation dynamics such as kinetic energy release (KER) is of great importance and can help to understand the processes occurring in atmospheric chemistry.

The KER of the de-nitrogenation channel of N_2O^{2+} induced in collisions with electrons,[7,10–12] highly charged ions (HCIs),[8,13] and intense infrared laser fields[5,14–16] have been extensively studied. Generally, the dissociation energy strongly depends on the molecular potential curves populated. Accordingly, the KER distributions are subject to projectile species and energies, and a large variety of spectra have been reported in literature.

In 1991, Eland and Murphy found that the peak of KER is around 7.2 ± 0.7 eV induced by 1300 eV electron impact.[10] At a much lower collision energy of 50 eV, the KER was found to be at 6.3 ± 1.0 eV.[11] For higher electron impact energies of 10 keV, two peaks in the KER distribution were identified.[7] These peaks are located at 4.0 ± 0.5 eV and 5.3 ± 0.6 eV with relative intensities of 58 : 42, respectively. Later, similar structures were also observed for 5 keV electron impact where the major peak was found at 6.6 ± 0.2 eV.[12]

After double ionization of N_2O molecules in intense infrared laser fields, the KER has been reported to be around 6.5 ± 2.0 eV,[14] 6.8 ± 2.0 eV,[15] and 6.8 eV[5] for different laser intensities. After absorptions of the single photons from

*Project supported by the National Key Research and Development Program of China (Grant No. 2017YFA0402300).
†Corresponding author. E-mail: zhangshf@impcas.ac.cn
‡Corresponding author. E-mail: x.ma@impcas.ac.cn
© 2020 Chinese Physical Society and IOP Publishing Ltd

the He II radiation (He IIα 30.4 nm, He IIβ 25.6 nm, etc.), the peaks were found to be centered around 6.4 ± 0.3 eV[17] and 6.3 ± 0.3 eV.[6] However, a different value of 7.2 ± 0.4 eV was reported for the shorter wavelength of 25.6 nm.[10] The dependence of the total kinetic energy of the de-nitrogenation process on the photon energy of synchrotron radiations was reported by Alagia *et al.*[18–20] It was also found that the photodissociation processes of N_2O^{2+} are dominated by the direct Coulomb explosion in the case of photon energies between ~ 35.5 eV and ~ 38.5 eV.[21]

While these studies generally contribute to our understanding of the dissociation dynamics, in the case of the double ionization by electrons, ions, and intense infrared laser fields, various states of N_2O^{2+} can be populated which can hardly be resolved in the KER spectra. Moreover, several electronic dissociation pathways are involved which can interfere, making an interpretation of the observed spectra even more complicated.

Very recently, the dissociation pathways of N_2O^{2+} induced by collisions between 5.7 keV/u Xe^{15+} and N_2O were distinguished.[8] In the work, the KER spectra showed some similarities to those of electron/photon impact, and the peak positions were found at 6.8 eV and 9.0 eV, respectively. It was concluded that the measured peak at 6.8 eV originates from two states: (a) the N_2O^{2+} ground state ($X^3\Sigma^-$) which dissociates to $N^+(^3P) + NO^+(^1\Sigma^+)$; (b) the metastable state ($1^3\Pi$) which decays radiatively to $X^3\Sigma^-$ and dissociates subsequently. The signature of the metastable ($1^3\Pi$) state could clearly be recognized from the long tail in the two-fragment time-of-flight coincidence spectrum.[21,22] A shoulder around 9.0 eV was attributed to N_2O^{2+} ($1^1\Pi$, $1^1\Sigma^-$) dissociating to $N^+(^1D) + NO^+(^1\Sigma^+)$ via the potential energy curve crossing of the $1^1\Pi$ and $1^1\Sigma^-$ states of N_2O^{2+}

In this paper, we report on the direct Coulomb explosion of N_2O^{2+} induced by the extreme ultraviolet photons at the energy of ~ 38.5 eV. In our study, the photon energy is selected right below the metastable threshold energy ($E_{\rm mth} = 38.5$ eV[22]), and therefore, the population of the metastable state ($1^3\Pi$) is effectively suppressed. Meanwhile the molecular ion can only be populated in a few states, which greatly simplifies the analysis of the dissociation pathways. The momenta of the fragment ions are recorded in coincidence with the laser pulse by employing the reaction microscope for each fragmentation event. In the time-of-flight (TOF) coincidence spectra of two fragments, different dissociation channels of N_2O^{2+} are resolved. The KER distributions of the de-nitrogenation channel and the corresponding dissociation pathways are discussed in detail.

2. Experimental setup

The experimental setup is shown in Fig. 1. Briefly, the Ti:sapphire laser system[23] generates laser pulses with a central wavelength of ~ 800 nm at 3 kHz repetition rate. For each pulse, the energy is ~ 5 mJ and the pulse duration is about 25 fs. This intense infrared laser beam is then focused into a 5-cm long, 150-μm-diameter hollow fiber filled with argon gas to generate extreme ultraviolet (EUV) light via high harmonic generation (HHG).[24–26] After the fiber, a set of grating and pinhole are used to spectrally select the EUV photons and the monochromatic photon energy is determined from the photoelectron spectra in single ionization of helium whose binding energy is about 24.6 eV. Eventually, EUV light of ~ 38.5 eV (25th harmonic) with a bandwidth of about 0.4 eV can be obtained and the flux converted from the photo diode is about 10^9–10^{10} photons/s. Such pulses are then guided through a vacuum beam line to the reaction chamber. The beam line is pumped down to 10^{-6} mbar to reduce the EUV absorption of the background molecules.

In the reaction chamber, the monochromatic EUV pulse is focused onto the target. The gas target is prepared with the N_2O gas of about 99.99% purity using the supersonic gas target method, where the stagnation pressure is set to 12 bars.[27] Meanwhile, the background pressure in the target chamber of reaction microscope[28–30] can be kept at a sufficiently low value of 10^{-9} mbar. After absorption of the EUV photon, one or two electrons are removed from N_2O molecule which dissociates into charged fragments due to the Coulomb repulsion. A uniform electrostatic field of ~ 105 V/cm is used to project the positively charged fragments to the recoil ion detector (see Fig. 1). The TOF and position information of each fragment are recorded event by event in list-mode form. The momentum of each fragment thus can be reconstructed in the off-line analysis procedures.

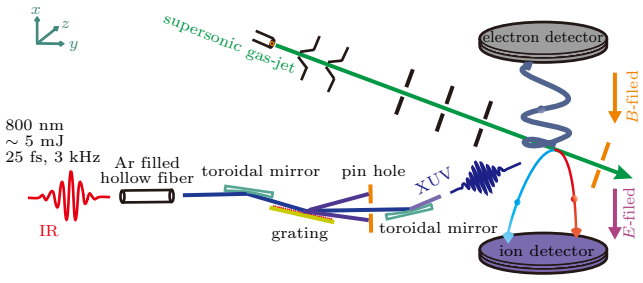


Fig. 1. Schematic view of the experimental setup (we note that the electron detector is not activated in the present work).

In the following discussion, the coordinate system is defined as following. The EUV light propagates in the Z direction, while the supersonic jet moves in the Y direction which is also the polarization direction of the EUV photons. Accordingly, the X direction is along the TOF spectrometer axis.

3. Results and discussion

Figure 2(a) represents the TOF spectra of all charged particles produced in the reaction chamber. For ions with zero momentum, the TOF T_R follows the relation

$$T_R \propto \sqrt{M/q},$$

where M and q are the mass and charge of the particle, respectively. At the photon energy of ~ 38.5 eV, one or two electrons can be removed from the N_2O molecule. Therefore, both N_2O^+, N_2O^{2+} molecular ions and their dissociation products are expected to be observed in our experiment. Indeed, N^+, O^+, N_2^+, NO^+, and N_2O^+ are clearly resolved in the TOF spectra. However, no stable N_2O^{2+} ions are observed in the TOF spectrum, which indicates that the molecular dication N_2O^{2+} produced after absorption of the EUV photon is subject to fast dissociation processes. In addition, one can also see that the ions from residual gas molecules like OH^+, H_2O^+, O_2^+, and Ar^+ also appear in the spectra. They are mainly from the gas influx from the EUV beam line.

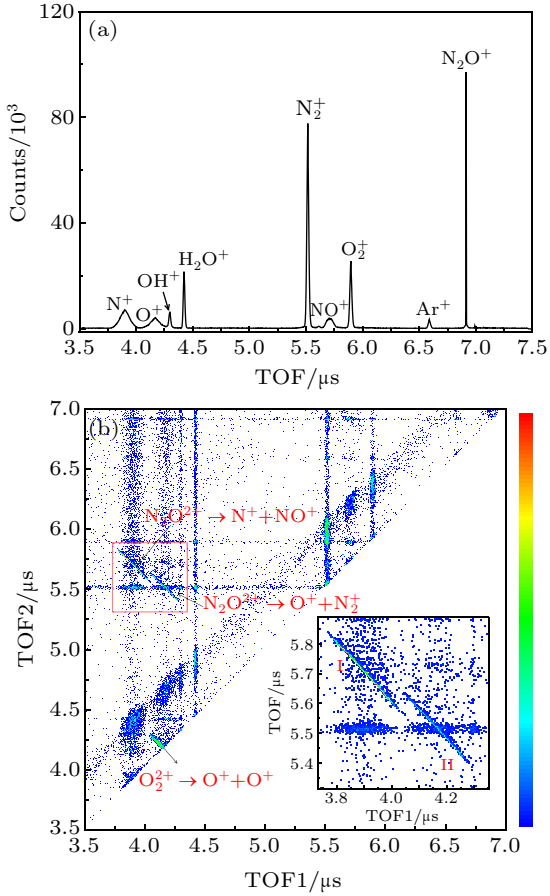


Fig. 2. (a) The TOF spectrum of recoil ions. (b) Two-dimensional TOF coincidence spectrum of charged fragments. Enlarged map is the Coulomb explosion process of N_2O^{2+}. The first slash line I centered at (3.90, 5.71) is from the de-nitrogenation photodissociation channel. Here, the x-axis value shows the TOF of N^+ fragments while the y-axis value shows the TOF of NO^+. The second slash line II at (4.17, 5.52) is the de-oxygenation photodissociation channel in which the x-axis value is the TOF of O^+ fragment and the y-axis value is that of N_2^+ fragment.

Figure 2(b) shows the ion–ion coincidence spectra from the fragments as measured at a photon energy of ~ 38.5 eV, where the x- and y-axis values represent the TOFs of the first fragment (TOF1) and the second one (TOF2), respectively. Neglecting the relatively small electron and photon momenta, the fragmentation could be treated as a two-body dissociation event, i.e., the two fragment ions fly back-to-back and share an equal amount of momentum. Consequently, distinct slash lines with a slope of about -1 appear in the coincidence spectrum. Whereas, the vertical and horizontal traces in the map represent false and random coincidences which can be easily discriminated in the present analysis and will not affect the quality of our results. In the spectra, two pronounced coincidence slash lines are clearly identified corresponding to the de-nitrogenation channel (I) and the de-oxygenation channel (II) (see the inset in Fig. 2(b)), respectively. The relative branching ratio of the two channels ($N^+ + NO^+/O^+ + N_2^+$) is about 7 : 2, in a good agreement with the previous results.[21] In the present work, we concentrate on the $N_2O^{2+} \rightarrow N^+ + NO^+$ channel. Comparing with the previous studies (for instance, see Refs. [5,8,10,12,21,31]) which reported a long tail extending from the $N^+ + NO^+$ coincidence trace in the ion–ion coincidence map, in contrast, the tail structure in our data can, if exists, hardly be observed.

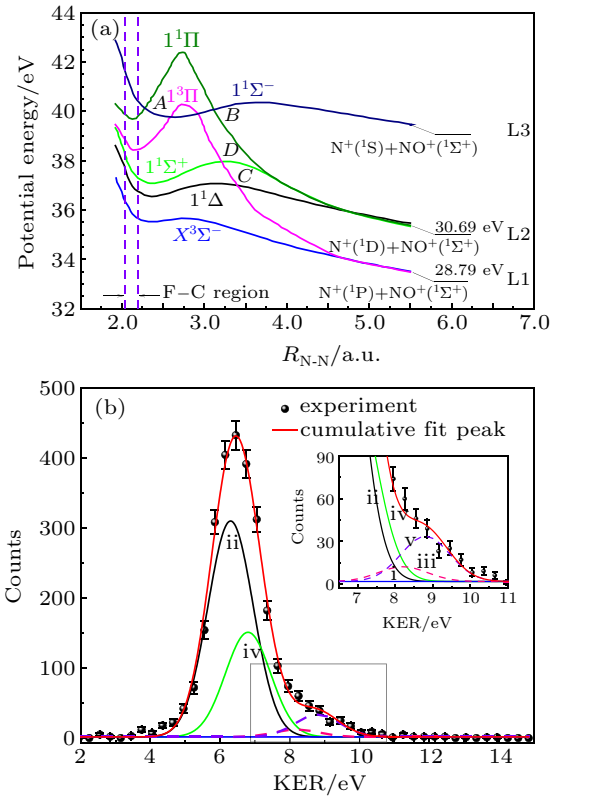


Fig. 3. (a) The potential energy curves of N_2O^{2+} given for the de-nitrogenation channel.[22] Vertical dashed lines indicate the Franck–Condon region. (b) The KER spectra of the de-nitrogenation process. The solid circles are experimental data, and the red solid lines are the fitting lines. The inset highlights the contributions from different pathways to the shoulder formation (see text).

The observed difference can be ascribed to the collisional population of the metastable $1^3\Pi$ state in the previous studies,[21,22] a channel which is energetically not allowed in our experiment. In the present work, we focus on the processes of two electrons removed from the outer-shell π-orbital of N_2O by absorption of a ~ 38.5 eV photon. The only accessible electronic states of the N_2O^{2+} dication are the $X^3\Sigma^-$, $1^1\Delta$, and $1^1\Sigma^+$ states (see Fig. 3(a)). Meanwhile, to a large extent the excitation to the metastable $1^3\Pi$ state is suppressed due to the limited photon energy. From all these possible electronic states, the N_2O^{2+} dication dissociates into two charged fragments and undergoes direct Coulomb explosions.[21]

The KER distribution of the $N_2O^{2+} \rightarrow N^+ + NO^+$ dissociation channel is shown in Fig. 3(b), which exhibits a major peak centered at 6.4 eV and a small shoulder located around 8.8 eV at the right wing of the major peak. Table 1 lists the KER values for the de-nitrogenation dissociation channel reported in literatures and results of our work. According to the potential energy curves (PECs) of N_2O^{2+} [22] shown in Fig. 3(a), N_2O^{2+} in states of $X^3\Sigma^-$, $1^1\Delta$, and $1^1\Sigma^+$ can dissociate through five different pathways: (i) direct dissociations of the ground state $X^3\Sigma^-$ to the first dissociation limit (L1) with the asymptotic potential level of $E_{L1} = 28.79$ eV,[9] (ii) direct dissociations from the $1^1\Delta$ state to the second dissociation limit (L2), whose asymptotic energy is $E_{L2} = 30.69$ eV.[9] (iii) predissociation from the $1^1\Delta$ state to $1^3\Pi$ via their potential curve crossing point (marked as *C*), (iv) direct dissociation of the $1^1\Sigma^+$ state to the second dissociation limit (L2), (v) predissociation from the $1^1\Sigma^+$ states to $1^3\Pi$ via their potential curve crossing point (marked as *D*). The corresponding KER peak values of these five channels are listed in Table 2 which are used as the Gaussian peak centers in the fitting procedure. Meanwhile, for all five Gaussian fittings, the same width of 1.3 eV is used in the first order approximation. The corresponding relative contributions from these processes are listed in Table 2.

Table 1. The KER peak values for $N_2O^{2+} \rightarrow N^+ + NO^+$ dissociation channel obtained in the present experiment and earlier reported experiments.

Projectiles	Condition	KER/eV
Electrons	1300 eV	7.2 ± 0.7[10]
	50 eV	6.3 ± 1.0[11]
	10 keV	4.0 ± 0.5, 5.3 ± 0.6[7]
	5 keV	6.6 ± 0.2[12]
HCIs	5.9 MeV/u Xe^{43+}	7.0[13]
	5.7 keV/u Xe^{15+}	6.8, 9.0[8]
Intense laser	795 nm, 100 fs, ~5 PW/cm^2	6.5 ± 2.0[14]
	800 nm, 60 fs, ~0.16 PW/cm^2	6.8 ± 2.0[15]
	750 nm, 4 fs, ~0.3 PW/cm^2	6.8[5]
Photons	40.8 eV	6.4 ± 0.3[17]
	12.4–51.7 eV	6.3 ± 0.3[6]
	48.4 eV	7.2 ± 0.4[10]
	~ 38.5 eV	6.4, 8.8[a]

[a]Present work.

Table 2. The KER values of de-nitrogenation channel derived from different dissociation pathways.

Dication state	Initial energy/eV	Dissociation limit	Asymptotic energy/eV	KER/eV	Relative contribution	Label
$X^3\Sigma^-$	35.825	$N^+(^3P) + NO^+(^1\Sigma^+)$ (L1)	28.79	7.035	2.6%	i
$1^1\Delta$	36.962	$N^+(^1D) + NO^+(^1\Sigma^+)$ (L2)	30.69	6.272	56.3%	ii
		$N^+(^3P) + NO^+(^1\Sigma^+)$ (L1)	28.79	8.172	4.4%	iii
$1^1\Sigma^+$	37.546	$N^+(^1D) + NO^+(^1\Sigma^+)$ (L2)	30.69	6.856	28.6%	iv
		$N^+(^3P) + NO^+(^1\Sigma^+)$ (L1)	28.79	8.756	8.1%	v

From the fitting results, we conclude that the major peak centered at 6.4 eV can be attributed to two processes: (i) the dominant photodissociation peak centered at 6.3 eV (black solid curve) which represents a direct decay from the $1^1\Delta$ state to the second dissociation limit of $N^+(^1D) + NO^+(^1\Sigma^+)$, (ii) the second peak at 6.8 eV (green solid curve) is assigned to the direct dissociation of the $1^1\Sigma^+$ state to the same dissociation limit (L2). Meanwhile, the contribution from the ground state $X^3\Sigma^-$ (blue solid curve, see Fig. 3(b) and Table 2) is negligibly small. These results indicate that the dication of N_2O^{2+} formed by absorption of one 38.5 eV photon is mainly populated in the $1^1\Delta$ and $1^1\Sigma^+$ states, and the direct dissociations from these states are the dominant decay processes. These populations are very similar to those observed previously in the double photoionization of N_2O by He II radiations at 30.4 nm[32] and 25.6 nm.[22] Whereas, in Refs. [5,8], the major peak centered around 6.8 eV (see Table 1) is attributed to both contributions from the direct dissociation of the ground state $X^3\Sigma^-$ and the decay of $1^3\Pi$ to $X^3\Sigma^-$ through fluorescence which consequently undergoes the Coulomb explosion.[20] Moreover, the dissociation of the $1^1\Delta$ and $1^1\Sigma^+$ states was not addressed.

Accordingly, the shoulder structure around 8.8 eV can be interpreted as follows. As pointed out above, with ~ 38.5 eV photon energy the electronic states of N_2O^{2+} are mainly populated to the $1^1\Delta$ and $1^1\Sigma^+$ states. Therefore, there is a good reason to believe that the shoulder structure is ascribed to the decay of the $1^1\Delta$ and $1^1\Sigma^+$ states of N_2O^{2+} to the first dissociation limit of $N^+(^3P) + NO^+(^1\Sigma^+)$. This dissociation takes place through the potential curve crossings with the $1^3\Pi$ state at *C* and *D* shown in Fig. 3(a). These pathways via *C* and *D* will produce dissociation energies of 8.2 eV (pink dashed curve) and 8.8 eV (purple dashed curve) as shown in Fig. 3(b), respectively. Besides, the direct decay from the $1^1\Delta$ states to

L2 is much stronger than the predissociation to L1. The first reason is that the vibrational states in $1^1\Delta$ are highly populated, and are very close or partly over the barrier. A second reason is that the crossing point (*C*) is outside the potential well, i.e., beyond the barrier. On the other hand, the predissociation of the $1^1\Sigma^+$ state via the crossing with $1^3\Pi$ state (*D*) is relatively stronger since the crossing is inside the well and bellow the barrier. Taking all the above factors into account, we can conclude that the main contribution to the shoulder structure is from the $1^1\Sigma^+$ states of N_2O^{2+} to the first dissociation limit of $N^+(^3P)+NO^+(^1\Sigma^+)$ with potential curve crossing of the $1^3\Pi$ state.

However, our results are different from the earlier results of Chen *et al.*[8] In their study, they used 5.7 keV/u Xe^{15+} beam ions to produce N_2O^{2+}, therefore, they observed a shoulder structure situated at 9.0 eV of the de-nitrogenation channel. This structure was explained by the population of the $1^1\Pi$ state in N_2O^{2+} which predissociates to the second dissociation limit (L2) of $N^+(^1D)+NO^+(^1\Sigma^+)$. This predissociation occurs through two crossing points of the potential energy curves, as shown by *A* and *B* in Fig. 3(a). The difference between our results and those in Ref. [8] is obvious since, in ion induced collisions all excited states might be populated while in photon impact situation, only few specific states can be populated due to the energy restriction.

4. Conclusion

The Coulomb explosion of N_2O^{2+} is studied with the reaction microscope double photoionization from N_2O by extreme ultraviolet photons at ~ 38.5 eV. The de-nitrogenation as well as the de-oxygenation channels are identified from the time-of-flight coincidence spectra. It is found that, in the de-nitrogenation channel, the N_2O^{2+} dications mainly dissociate from the $1^1\Delta$ and $1^1\Sigma^+$ states. In the KER spectra, a main peak centered at 6.4 eV with a shoulder towards higher energies is observed. Further studies show that the major peak is derived from the direct dissocaition of N_2O^{2+} from the $1^1\Delta$ and $1^1\Sigma^+$ potential curve to $N^+(^1D)+NO^+(^1\Sigma^+)$ (the second dissociation limit L2). The shoulder is originated from the dissociation of N_2O^{2+} from the $1^1\Delta$ and $1^1\Sigma^+$ states to $N^+(^3P)+NO^+(^1\Sigma^+)$ (the first dissociation limit L1) via the crossing of the $1^3\Pi$ state potential energy curves. Our work shows that the table-top monochromatic EUV beam line provides great advantages in detailed studies of the electronic states and dissociation dynamics involved in photo-ionization of molecular systems.

Acknowledgment

The authors thank D. B. Qian and D. Fischer for helpful discussions.

References

[1] Forster B P 2007 *Climate Change 2007: The Physical Science Basis* (New York: Cambridge University Press) pp. 1–21

[2] Ravishankara A R, Daniel J S and Portmannand R W 2009 *Science* **326** 123

[3] Thompson R L, Lassaletta L, Patra P K, Wilson C, Wells K C, Gressent A, Koffi E N, Chipperfield M P, Winiwarter W, Davidson E A, Tian H and Ganadell J G 2019 *Nat. Clim. Chang.* **9** 993

[4] Kotsina N, Kaziannis S, Danakas S and Kosmidis C 2013 *J. Chem. Phys.* **139** 104313

[5] Kübel M, Alnaser A S, Bergues B, Pischke T, Schmidt J, Deng Y, Jendrzejewski C, Ullrich J, Paulus G G, Azzeer A M, Kleineberg U, Moshammer R and Kling M F 2014 *New J. Phys.* **16** 065017

[6] Price S D, Eland J H D, Fournier P G, Fournier J and Millie P 1988 *J. Chem. Phys.* **88** 1511

[7] Bhatt P, Singh R, Yadav N and Shanker R 2012 *Phys. Rev. A* **86** 052708

[8] Chen L, Shan X, Zhao X, Zhu X L, Hu X Q, Wu Y, Feng W T, Guo D L, Zhang R T, Gao Y, Huang Z K, Wang J G, Ma X W and Chen X J 2019 *Phys. Rev. A* **99** 012710

[9] Murphy R and Eberhardt W 1988 *J. Chem. Phys.* **89** 4054

[10] Eland J H D and Murphy V J 1991 *Rapid Commun. Mass Spectrom.* **5** 221

[11] Love N A and Price S D 2004 *Phys. Chem. Chem. Phys.* **6** 4558

[12] Khan A and Misra D 2016 *J. Phys. B: At. Mol. Opt. Phys* **49** 055201

[13] Siegmann B, Werner U, Lutz H and Mann R 2003 *GSI Scientific Report 2002* (Darmstadt: GSI), p. 100

[14] Hishikawa A, Iwamae A, Hoshina K, Kono M and Yamanouchi K 1998 *Res. Chem. Intermed.* **24** 765

[15] Ueyama M, Hasegawa H, Hishikawa A and Yamanouchi K 2005 *J. Chem. Phys.* **123** 154305

[16] Ma J Y, Lin K, Ji Q Y, Zhang W B, Li H X, Sun F H, Qiang J J, Lu P X, Li H, Gong X C and Wu J 2019 *Chin. Phys. B* **28** 093301

[17] Curtis D and Eland J 1985 *Int. J. Mass Spectrom. Ion Processes* **63** 241

[18] Alagia M, Candori P, Falcinelli S, Lavollée M, Pirani F, Richter R, Stranges S and Vecchiocattivi F 2007 *J. Chem. Phys.* **126** 201101

[19] Falcinelli S, Rosi M, Candori P, Vecchiocattivi F, Farrar J M, Pirani F, Balucani N, Alagia M, Richter R and Stranges S 2014 *Planet Space Sci.* **99** 149

[20] Falcinelli S, Pirani F, Alagia M, Schio L, Richter R, Stranges S, Balucani N and Vecchiocattivi F 2016 *Atmosphere* **7** 112

[21] Alagia M, Candori P, Falcinelli S, Lavollée M, Pirani F, Richter R, Stranges S and Vecchiocattivi F 2006 *Chem. Phys. Lett.* **432** 398

[22] Taylor S, Eland J H D and Hochlaf M 2006 *J. Chem. Phys.* **124** 204319

[23] KMLABS https://www.kmlabs.com/

[24] L'Huillier A and Balcou P 1993 *Phys. Rev. Lett.* **70** 774

[25] Gagnon E, Sandhu A S, Paul A, Hagen K, Czasch A, Jahnke T, Ranitovic P, Cocke C L, Walker B, Murnane M M and Kapteyn H C 2008 *Rev. Sci. Instrum.* **79** 063102

[26] Niu Y, Liang H J, Liu Y, Liu F Y, Ma R and Ding D J 2008 *Chin. Phys. B* **26** 074222

[27] Schmidt H T, Cederquist H, Schuch R, Bagge L, Källberg A, Hilke J, Rensfelt K G, Mergel V, Achler M, Dörner R, Spielberger L, Jagutzki O, Schmidt-Böcking H, Ullrich J, Reich H, Unverzagt M, Schmitt W and Moshammer R 1997 *Hyperfine Interact.* **108** 339

[28] Ullrich J, Moshammer R, Dorn A, Dörner R, Schmidt L Ph H and Schmidt-Böcking H 2003 *Rep. Prog. Phys* **66** 1463

[29] Ma X W, Zhang R T, Zhang S F, Zhu X L, Feng W T, Guo D L, Li B, Liu H P, Li C Y, Wang J G, Yan S C, Zhang P J and Wang Q 2011 *Phys. Rev. A* **83** 052707

[30] Guo D L, Ma X W, Feng W T, Zhang S F and Zhu X L 2012 *Acta Phys. Sin.* **60** 11341 (in Chinese)

[31] Zhou X, Ranitovic P, Hogle C W, Eland J H D, Kapteyn H C and Murnane M M 2012 *Nat. Phys.* **8** 232

[32] Eland J H 2003 *Chem. Phys.* **294** 171